Received: July 21, 2017 Revised: March 5, 2018 Accepted: March 9, 2018

(onlinelibrary.wiley.com) DOI: 10.1111/ner.12786

Automatic M1-SO Montage Headgear for Transcranial Direct Current Stimulation (TDCS) Suitable for Home and High-Throughput In-Clinic Applications

Helena Knotkova, PhD*†; Alexa Riggs, MPH*; Destiny Berisha, BEngc*‡; Helen Borges, MS‡; Henry Bernstein, MS‡; Vaishali Patel, BE*; Dennis Q. Truong, PhDc‡; Gozde Unal, PhDc‡; Denis Arce, BE§; Abhishek Datta, PhD§; Marom Bikson, PhD‡

Objectives: Non-invasive transcranial direct current stimulation (tDCS) over the motor cortex is broadly investigated to modulate functional outcomes such as motor function, sleep characteristics, or pain. The most common montages that use two large electrodes (25–35 cm^2) placed over the area of motor cortex and contralateral supraorbital region (M1-SO montages) require precise measurements, usually using the 10–20 EEG system, which is cumbersome in clinics and not suitable for applications by patients at home. The objective was to develop and test novel headgear allowing for reproduction of the M1-SO montage without the 10–20 EEG measurements, neuronavigation, or TMS.

Materials and Methods: Points C3/C4 of the 10–20 EEG system is the conventional reference for the M1 electrode. The headgear was designed using an orthogonal, fixed-angle approach for connection of frontal and coronal headgear components. The headgear prototype was evaluated for accuracy and replicability of the M1 electrode position in 600 repeated measurements compared to manually determined C3 in 30 volunteers. Computational modeling was used to estimate brain current flow at the mean and maximum recorded electrode placement deviations from C3.

Results: The headgear includes navigational points for accurate placement and assemblies to hold electrodes in the M1-SO position without measurement by the user. Repeated measurements indicated accuracy and replicability of the electrode position: the mean [SD] deviation of the M1 electrode (size 5 × 5 cm) from C3 was 1.57 [1.51] mm, median 1 mm. Computational modeling suggests that the potential deviation from C3 does not produce a significant change in brain current flow.

Conclusions: The novel approach to M1-SO montage using a fixed-angle headgear not requiring measurements by patients or caregivers facilitates tDCS studies in home settings and can replace cumbersome C3 measurements for clinical tDCS applications.

Keywords: At-home tDCS, fixed-angle M1 headgear, computational modeling, noninvasive neurostimulation, transcranial direct current stimulation (tDCS)

Conflict of Interest: Drs. Bikson and Datta have equity in Soterix Medical Inc. The City University of New York has patents on brain stimulation with Drs. Bikson, Truong, and Datta as inventors. Dr. Arce is an employee of Soterix Medical. The remaining authors do not have conflicts of interest to disclose.

INTRODUCTION

Transcranial direct current stimulation (tDCS) is a method of non-invasive neurostimulation utilizing low-intensity electrical current passed across the brain, typically with two large (25–35 cm^2) saline-soaked sponge electrodes (anode and cathode) placed on the subject's head (1–15). The position of tDCS electrodes on the scalp governs the pattern of underlying brain current flow, and which brain regions are stimulated (7,8). The position of electrodes on the scalp is therefore a critical factor (16–20).

tDCS stimulation of the motor cortex using a montage with electrodes placed on the surface of the head over the area of motor cortex and contralateral supraorbital region (M1-SO montage) has been frequently used in both research and clinical settings, not only for

Address correspondence to: Helena Knotkova, PhD, MJHS Institute for Innovation in Palliative Care, 39 Broadway, 3rd Floor, New York, NY 10006, USA. Email: HKnotkov@mjhs.org

* MJHS Institute for Innovation in Palliative Care, New York, NY, USA;
† Department of Family and Social Medicine, Albert Einstein College of Medicine, Bronx, NY, USA;
‡ Department of Biomedical Engineering, The City College of New York of CUNY, New York, NY, USA; and
§ Soterix Medical Inc., New York, NY, USA

For more information on author guidelines, an explanation of our peer review process, and conflict of interest informed consent policies, please go to http://www.wiley.com/WileyCDA/Section/id-301854.html

Source(s) of financial support: None

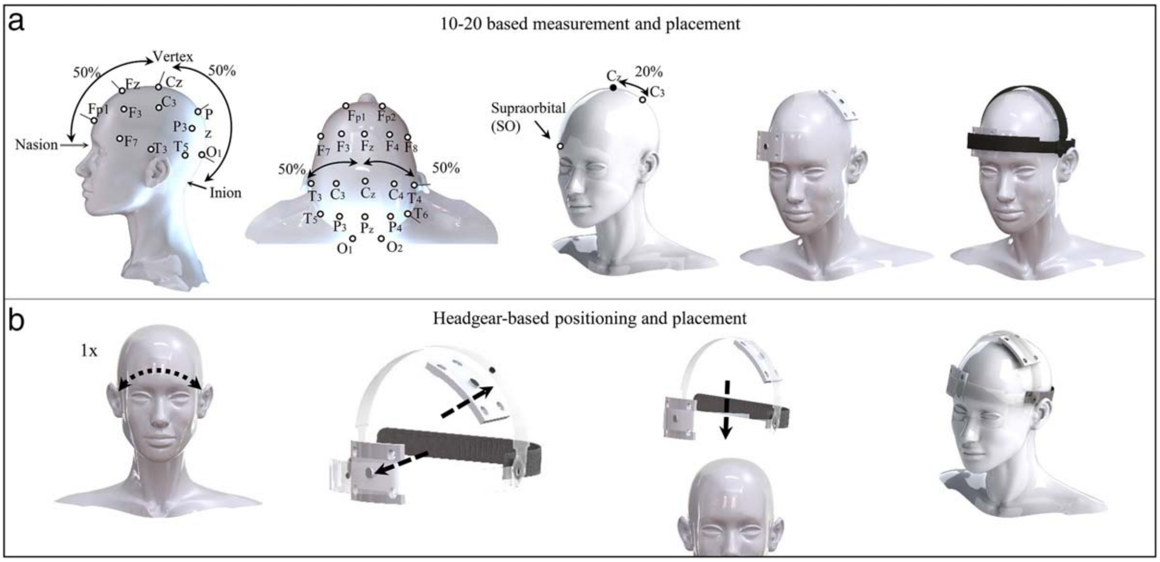

Figure 1. Schematic of conventional M1-SO montage using manual 10–20 EEG-based measurements, and straps (a), and the proposed automatic headgear-based positioning (b). a. Left to Right: The protocol for conventional M1-SO positioning involves at each session using a tape-measure and a marker to identify the vertex (the CZ point) using two measurements, a third measurement to identify and mark C3, whereas SO is identified ad hoc. The electrodes are manually positioned over the marked scalp, and finally two or more elastic bands are wrapped around the scalp to hold the electrodes. b. Left to Right: The proposed automatic method for M1-SO positioning requires a one-time measurement to select the headgear size; the electrodes are then connected to the headgear at fixed positions, and the entire headgear with electrodes is then lowered on the head, where the headgear ensures precise electrode positioning and reliable skin contact. [Color figure can be viewed at wileyonlinelibrary.com]

modulation of motor function (21–24), but also when aiming for pain relief (25–30), or for modulation of sleep characteristics (31,32). To date, the M1 electrode position in the M1-SO montage can be determined using one of the following methods: 1) direct determination of the “hot spot” via evaluation of motor evoked potentials (MEPs) induced by the transcranial magnetic stimulation (TMS) of the motor area, with or without support by neuronavigational systems (1,33); or 2) using the electrode position measurements delineated by the International 10–20 EEG system (Fig. 1a), which require determining distances between the 10–20 anatomical landmarks (inion, nasion, vertex, preauricular points) in order to determine the C3 (or C4) point that corresponds with 20% of preauricular distance in coronal plane, measured from the vertex toward the preauricular point (34).

In research and clinical settings, the TMS approach is complex and costly, and has been used only in a minority of the overall pool of M1-SO tDCS applications. The more frequently used International 10–20 EEG system is cumbersome and prone to substantial operator error, especially under conditions of high throughput. Moreover, neither of these methods is suitable for replication in home settings. The problem of how to easily and reliably determine the electrode position and affix the electrode on the patient’s/user’s head at home represents a substantial barrier to implementing a novel at-home tDCS approach (35) which is much needed in order to decrease burden associated with facility-based tDCS applications. Thus, we aimed to develop and test a novel approach allowing for reproduction of M1-SO tDCS montage suitable for home settings by lay users, such as patients or their informal caregivers, without 10–20 EEG measurements for electrode placement.

METHODS

Approach

The 10–20 EEG positioning system was taken as a standard for determining the M1 electrode scalp target (Fig. 1a). Specifically, C3 on the left hemisphere and C4 on the right represent the reference points over which a large tDCS electrode is centered in the conventional M1-SO montage. Given the position of C3 (C4), we have aimed for a solution utilizing a fixed-angle approach for headgear that would closely match the C3 (C4) standard without the actual measurement and would allow for fail-safe electrode insertion (Fig. 1b).

The guiding imperatives for the headgear design were accuracy, replicability, and ease of use. To assure that the final design solution met the guiding imperatives, the prototype of the headgear was evaluated at repeated placements of the headgear on the head in a sample of 30 subjects, and by computational modeling, as specified later.

Subjects

The sample consisted of 30 volunteers (14 M, 16 F) recruited at the City College of New York of City University of New York. Inclusion criteria required subjects to be 18 years of age or older. The participants provided verbal consent to participate in the accuracy and replicability assessment of the headgear, as described later. Each subject was required to participate in one 30- to 45-min long session. The procedure was approved by the CUNY IRB.

Accuracy and Replicability Assessment

The head circumference of each subject was measured in order to determine the appropriate size of the headgear to be used (S: 52–55.5 cm, M: 55.5–58.5 cm, L: 58.5–62 cm, XL: 62–65 cm). Appropriate measurements for the M1-SO position, as well as deviations from the ideal C3 position, were determined manually by a trained tDCS assistant using the measurement protocol for the 10–20 EEG system. The total of 600 repeated placements were performed, 20 placements for each subject under two conditions: 1) “assisted placement”—the headgear was placed on the subject’s head by a designated member of the study team (ten repetitions/subject); 2) “self-placement”—the headgear was placed on the head by the subject utilizing navigational marks on the headgear viewed in a mirror (again ten repetitions/subject). In both assisted and self-placement conditions, the researcher measured the distance between the target point initially marked via manual 10–20 EEG measurements and where the corresponding electrode in the headgear laid after each repetition.

Data Analysis

Independent variables included size of the headgear and placement condition (self-placement vs. assisted placement). Size was treated as a categorical variable and included three levels: small, medium, and large/extra-large. Large and extra-large were collapsed for computations due to rarity of size extra-large. For subjects with head circumference on the border between headgear size selection (e.g., 55.5 cm between sizes S and M), the headgear size that resulted in the best fit (based on sponge contact with the head and subject comfort) was selected and only this size was used in the analysis. The dependent variable was the measurement in mm from the ideal position of C3, and the error values (misplacements in anterior or posterior direction from C3) were treated as an absolute value.

SPSS version 24 was used for all analyses, including descriptive statistics and bivariate analysis. Descriptive statistics were conducted to report the mean (SD), median, minimum, and maximum for self- vs. assisted placement. The Shapiro-Wilk test was conducted to test for normality, and as measurements were not normally distributed nonparametric tests were employed for further analysis. Wilcoxon Rank-Sum Test was used as a nonparametric alternative to the paired sample's T test to compare means across placement conditions. The Kruskal-Wallis test was used as a nonparametric alternative to the ANOVA test to compare means across different sizes.

Mean deviation from the C3 position and maximum error of placement then served as the entry parameters for computational modeling in order to estimate any potential changes in the brain current flow.

Computational Modeling

Finite element models of M1-SO stimulation were solved comparing C3 electrode placement methods. Previously modeled reference data (36) were used as a template for a magnetic resonance imaging (MRI)-derived finite element modeling emission microscopy (FEM) model. High resolution (1 mm^3) MRIs were segmented into seven conductive tissue regions (skin, fat, skull, cerebrospinal fluid, gray matter, white matter, and air) (37). The position of the C3 point was located in the model using a standard procedure as delineated by 10–20 EEG measurement guide and described elsewhere (38). Square (5 $\times$ 5 cm^2) saline-soaked sponges and electrodes were modeled (39) and centered directly over the calculated C3 location and above the contralateral supraorbital (SO) region. Following the norm in clinical practice, the SO location was determined visually to be on the forehead, above the brow, and away from the eyes. The mean and maximum error of placement noted during the repeated placements of the prototype were modeled as a displacement of the ideal C3 location. A voxel-based adaptive meshing algorithm (Simpleware, Exeter, UK) was used to generate volume meshes consisting of more than 10 million elements. Boundary conditions (1 mA inward current at the anode and $V = 0$ at the cathode) were applied to electrostatic field conditions ($\nabla.\ (\sigma \nabla V) = 0$), which was solved for voltage and electric field. Cortical electric field was plotted as a representation of stimulation (3,4).

This evaluation protocol was designed with the objective to determine if the novel headgear supported precise placement if positioned following instructions and navigational marks on the headgear. The further question of user's "case-specific adherence to the instructions" by practitioners and patients is addressed in the Discussion; but in principle a pre-set electrode position headgear with snap electrodes presents less complexity and potential for error than manually inter-connected rubber bands and electrodes with multistep preparation.

RESULTS

The final design (Fig. 2a–d) for the M1-SO montage without the 10–20 EEG measurements includes a headgear with a connected horizontal (frontal) and vertical (coronal) strap connection in a three-dimensional angle that is closed in an orthogonal junction of both strap planes. This replicates a constant typical angle formed between the horizontal and the vertical plane for the M1-SO montage guided by the 10–20 EEG system. Each strap bends to contour the head and includes assemblies to fix electrode position, accommodating either snap-on pre-moisturized electrodes or conventional saline-soaked ones (Fig. 2c,d), of size 5 $\times$ 5 cm or 5 $\times$ 7 cm. The headgear was designed in four sizes—S, M, L, and XL—to accommodate for head sizes with preauricular-point distances ranging from 32 cm (S) to 38 cm (XL), and has additional elastic elements in the form of small diamond-shaped cuts on both frontal and coronal straps (Fig. 2a) facilitating appropriate fit within sizes.

The horizontal strap has a center-point mark for visual adjustment in the horizontal plane, with the headgear position otherwise self-correcting when placed snuggly on the head. The horizontal strap has two possible positions for the SO electrode from the fixed center point, to allow for customization of the SO electrode position due to variations in facial shape, and is designed to accommodate only one of those positions after adjustment, so that a misplacement of the SO electrode by the user in home settings is unlikely.

The vertical strap accommodates a single M1 electrode with the targeted center corresponding with the virtual position of C3 on the left hemisphere (or C4 on the right hemisphere) at the distance of 6.5 cm from the vertex point of the headgear for the S size (6.5 cm $\sim$ 20% of 32–33 cm reflecting preauricular-point distance for which the S size is fitted), and 7.5 cm for the XL size (37–38 cm preauricular-point distance). The selection of the headgear requires a single fitting session to select the size and the SO electrode position, which can be done when the headgear is dispensed to the user.

An assessment of the total of 600 repeated electrode placements using the size-fitted headgear in 30 subjects (size S $n = 8$; M $n = 16$; L = 5; XL = 1) with ten repeated measurements under each of the two conditions (self-placement and assisted placement) yielded 160 repeated placements for headgear of size S, 320 placements for size M, and 120 placements for size L/XL. The overall evaluation indicated accuracy and replicability of the electrode position over C3 using the headgear, as compared to the manually determined C3: the overall mean [SD] deviation of the center of the electrode from C3 during repeated placement of the headgear on the head was 1.57 [1.51] mm, median 1 mm, range 0–7 mm. The errors included both anterior and posterior displacements and no systematic direction of the errors was noted. The outlier four measurements of 7 mm deviation were not excluded from computations and served in the computational model as the value of maximal error of placement. There was no significant difference of displacement across

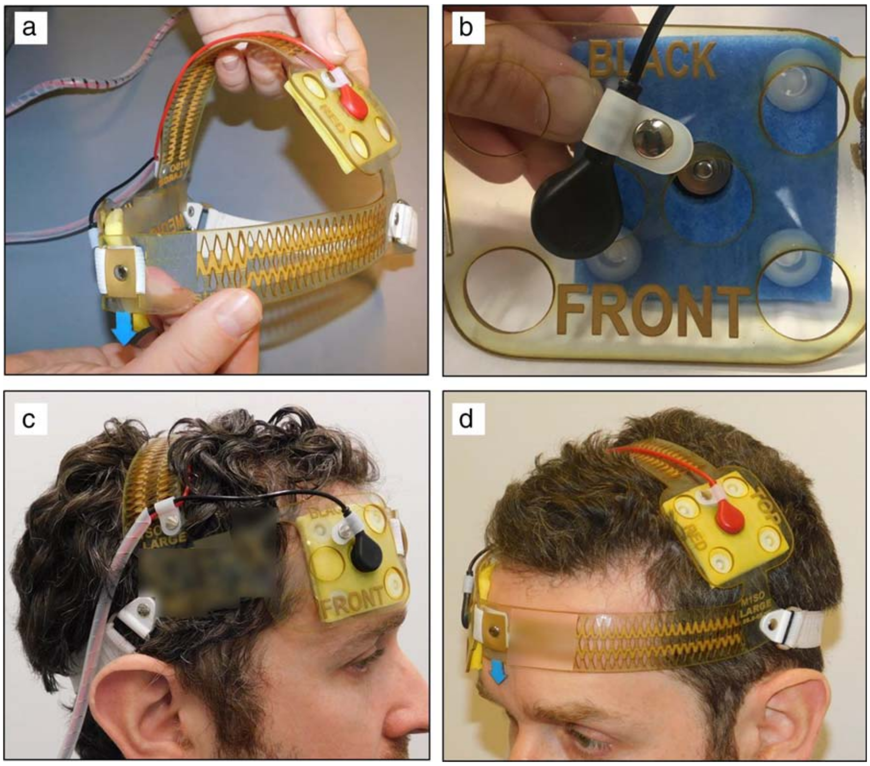

Figure 2. Images of the automatic tDCS headgear suitable for home use and high-throughput clinic use. The headgear (a) is size-fitted (S, M, L, XL) and has additional elastic elements in the form of small diamond-shaped cuts on both frontal and coronal straps facilitating appropriate fit within sizes. The headgear is labeled and allows for electrode positioning in only the set locations. The center point (blue arrow) supports accurate self-placement by user. The headgear accommodates either snap-on pre-moisturized electrodes (b) or conventional saline-soaked ones (not shown). The center point (blue arrow) supports accurate self-placement by user. The SO electrode is positioned using a frontal strap (c) while the M1 electrode is position via a coronal strap (d). [Color figure can be viewed at wileyonlinelibrary.com]

sizes of headgear ($p = 0.665$), indicating that the headgear size had no significant effect on accuracy of the placement. There was a significant difference ($p = 0.001$) between the self-placement and proxy-assisted placement: mean [SD] 1.76 mm [1.61], median 1 range 0–7 mm; and 1.38 mm [1.38], median 1, range 0–6 mm, respectively.

The computational modeling (Fig. 3a–c) predicted that the potential displacement of the M1 electrode of size 5 × 5 cm from the ideal position (C3) by the mean 1.57 mm, or by the outlying recorded maximal error of placement of 7 mm, does not significantly change the brain current flow. In all cases, comparable peak electric field magnitude and distributions were predicted, with a characteristic

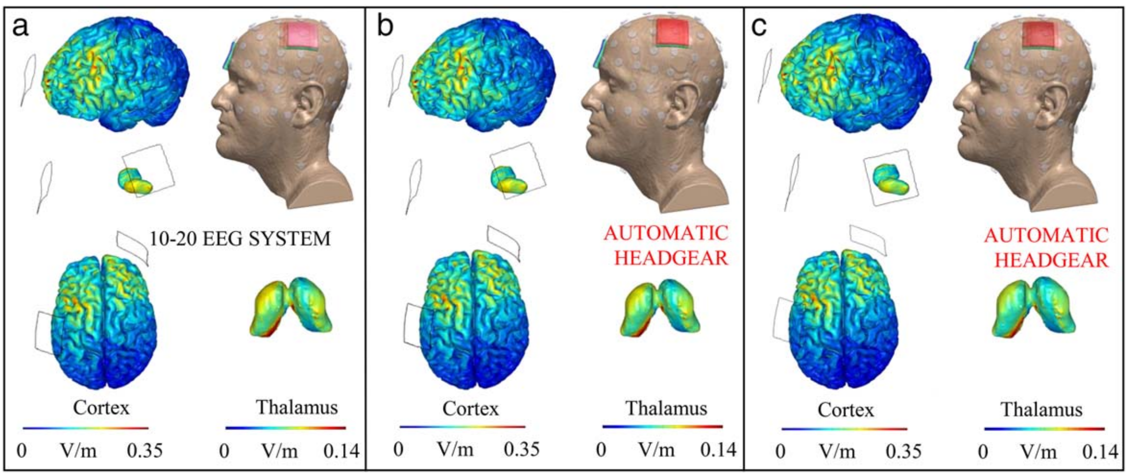

Figure 3. An MRI-derived computational model of brain current flow using the M1-SO montage. a. Ideal position based on the International EEG 10–20 positioning system. b. M1 electrode displacement by the mean error, using the headgear. c. M1 electrode displacement by the maximum error for the headgear. Consistent with previous simulations and recording, the M1-SO montage produces diffuse current flow across the frontal cortex and deep brain regions. Using the automatic headgear, under average or maximal recorded displacement from the ideal position, the resulting brain current flow patterns are not significantly changed. Electric field magnitude for all M1 electrode positions resulted in the comparable EF scale: 0–0.35 V/m on the cortex and 0–0.14 V/m at the thalamus. [Color figure can be viewed at wileyonlinelibrary.com]

clustering of electric field hotspots in gyri between stimulation electrodes. Previous studies have predicted much greater (twofold) differences in cortical electric field magnitude due to inter-individual anatomical variability (36,37). Variability due to electrode placement error is comparatively small.

DISCUSSION

In the presented work, we have developed a tDCS headgear allowing for reliable electrode placement in the M1-SO montage that is suitable for home settings or high-throughput clinics. At-home tDCS is needed not only for patients with low functional status or disabilities, but to broadly reduce costs driven by the tDCS personnel time and effort, and to enhance subject retention and compliance with tDCS interventions that involve repeated sessions spanning over weeks. For the objectives of this study, the headgear was positioned by a subject or proxy, following the guidelines for headgear placement (Figs. 1 and 2), establishing that using the headgear as prescribed supports precise positioning. The results indicated that accuracy of the placement was maintained across the headgear sizes. The results also suggested that the accuracy of placement further increased under the condition of assisted placement. However, the observed difference of the mean misplacement by 1.76 mm under self-placement as compared to 1.38 mm under assisted placement, although statistically significant, is minor when considered in the overall context of tDCS that utilizes large electrodes and generates currents with low spatial specificity.

We did not assess adherence to the headgear placement instructions in the sense of reliability in a subject population or course of treatment, including for home use. In translating tDCS to home use, the novel headgear represents a technological *prerequisite* for reproducible tDCS applications. It is of crucial importance that tDCS deployment to lay users, such as patients or their family caregivers, includes thorough subject selection and comprehensive training, paired with sufficient resources for adherence and outcome monitoring, in accordance with good practices and guidelines for tDCS in home settings (35). Further, specific training plans must reflect user-specific limitations in both physical and cognitive domains. For this reason, compliance in the headgear use must be tested in an application-specific manner. Nonetheless, we anticipate increased reproducibility compared to conventional protocols using sets of rubber bands. Indeed, an electrode drift from the proper position during tDCS stimulation have been frequently noted in the use of rubber bands (19), and novel solutions for a tDCS headgear equipment may help address this problem.

At any point or setting, reliability and tolerability of tDCS application should not be compromised. Central to both is electrode positioning, which is determined by electrode headgear. Headgear and protocols developed for trained operators, including 10–20 EEG measurements and elastic bands, are cumbersome for home use. Other tools, such as TMS and neuronavigation used for the electrode placement in medical centers are completely excluded from home use. The general principle of headgear suitable for home use is to facilitate reproducible placement of the electrodes within acceptable tolerances, after reasonable low-burden training.

The exemplary case here reproduced the common M1(C3)-SO montage with sufficient precision, not significantly altering resulting brain current flow, as confirmed by computer stimulation. Reproducible performance is achieved through a single adjustment where headgear size (S, M, L, XL) and SO-electrode increment are set, after which the headgear accepts electrodes in only this pre-set position. The headgear is designed to allow attachment of electrodes. The headgear and electrodes can then be self-applied on the head using basic center-point mark on the headgear. Across head sizes, the M1 electrode was positioned by users within the median distance of 1 mm from C3. Given the size of the electrode (5×5 cm), this deviation is minimal and indeed did not alter predicted brain current flow (on an absolute scale $<5\%$ (36), or as compared to $>200\%$ inter-individual difference (4)).

The verified precision was achieved by using natural articulation of the headgear placed on the head with triangulation based on the horizontal and coronal headgear strap; the three-dimensional angle between the straps, curvature of the straps, and fixed position of electrodes along the straps provides accuracy.

The principle of triangulation can be generalized to various headgear, electrode, and connector design, as long as the essential geometric features are maintained. A further important feature is the combination of elasticity and stiffness to ensure an even and secure position of the electrode against the skin, verified by inspection and impedance testing. Any headgear should not obscure electrode placement or encourage fluid spread between electrodes; for this reason, elastic caps known from EEG practice are contraindicated.

Our headgear design and this report do not address other essential features or guidelines pertaining to at-home tDCS that relate to stimulation hardware and protocols, such as dose control or compliance monitoring (35). Headgear design is a necessary but not a sufficient component.

Our approach approximates the C3 point. Based on our modeling, we predict that small variation in the resulting position may not significantly affect brain current flow. Our approach to using the headgear itself as the measurement/positioning system is analogous to prior work optimized for DLPFC tDCS (so called "OLE" montage (40)); a difference in the OLE montage is that it was designed to optimize brain current flow rather than approximate any given EEG 10–20 placement. This report thus presents the first verified design for tDCS-placement headgear that provides remarkable precision and facilitates the development of similar headgear for other EEG 10–20 based montages. Such headgear will support the rational and safe transition of tDCS to home use and may be adopted in clinics where it would reduce operator burden and potential for errors. The use of this novel headgear, however, does not replace/negate the need for proper user training and monitoring, and further evaluations of the headgear in various tDCS populations of potential users are warranted.

Acknowledgment

The authors would like to thank Ms. Shelita Clark for administrative assistance with preparation of the manuscript.

Authorship Statements

Drs. Knotkova, Bikson, Arce, Datta and Mr. Bernstein and Ms. Riggs contributed to the development of design, technical solution, and evaluation of the novel headgear. Ms. Berisha and Borges-Delfino-De-Souza contributed to data collection with healthy volunteers. Computational modeling was conducted by

Mr. Truong and statistical analysis was performed by Ms. Patel and Ms. Riggs. Ms. Unal, Riggs, and Patel and Mr. Truong designed figures. Drs. Knotkova and Bikson prepared the manuscript with important intellectual input from the rest of the team. All authors approved the final manuscript.

How to Cite this Article:

Knotkova H., Riggs A., Berisha D., Borges H., Bernstein H., Patel V., Truong D.Q., Unal G., Arce D., Datta A., Bikson M. 2018. Automatic M1-SO Montage Headgear for Transcranial Direct Current Stimulation (TDCS) Suitable for Home and High-Throughput In-Clinic Applications. Neuromodulation 2018; E-pub ahead of print. DOI:10.1111/ner.12786

REFERENCES

1. Nitsche MA, Paulus W. Excitability changes induced in the human motor cortex by weak transcranial direct current stimulation. *J Physiol* 2000;527:633–639.
2. Bindman LJ, Lippold OC, Redfearn JW. The action of brief polarizing currents on the cerebral cortex of the rat (1) during current flow and (2) in the production of long-lasting after-effects. *J Physiol* 1964;172:369–382.
3. Bikson M, Inoue M, Akiyama H et al. Effects of uniform extracellular DC electric fields on excitability in rat hippocampal slices in vitro. *J Physiol (Lond)* 2004;557:175–190.
4. Rahman A, Reato D, Arlotti M et al. Cellular effects of acute direct current stimulation: somatic and synaptic terminal effects. *J Physiol (Lond)* 2013;591:2563–2578.
5. Nitsche MA, Cohen LG, Wassermann EM et al. Transcranial direct current stimulation: state of the art. *Brain Stimul* 2008;1:206–223.
6. Batsikadze G, Moliadze V, Paulus W, Kuo MF, Nitsche MA. Partially non-linear stimulation intensity-dependent effects of direct current stimulation on motor cortex excitability in humans. *J Physiol* 2013;591:1987–2000.
7. Polanía R, Paulus W, Nitsche MA. Modulating corticostriatal and thalamocortical functional connectivity with transcranial direct current stimulation. *Hum Brain Mapp* 2012;33:2499–2508.
8. DaSilva AF, Mendonca ME, Zaghi S et al. TDCS-induced analgesia and electrical fields in pain-related neural networks in chronic migraine. *Headache* 2012;52: 1283–1295.
9. Monte-Silva K, Kuo MF, Hessenthaler S et al. Induction of late LTP-like plasticity in the human motor cortex by repeated non-invasive brain stimulation. *Brain Stimul* 2013;6:424–432.
10. Nitsche MA, Kuo MF, Karrasch R, Wächter B, Liebetanz D, Paulus W. Serotonin affects transcranial direct current-induced neuroplasticity in humans. *Biol Psychiatry* 2009; 66:503–508.
11. Nitsche MA, Grundey J, Liebetanz D, Lang N, Tergau F, Paulus W. Catecholaminergic consolidation of motor cortical neuroplasticity in humans. *Cereb Cortex* 2004;14: 1240–1245.
12. Nitsche MA, Jaussi W, Liebetanz D, Lang N, Tergau F, Paulus W. Consolidation of human motor cortical neuroplasticity by D-cycloserine. *Neuropsychopharmacol* 2004;29:1573–1578.
13. Nitsche MA, Liebetanz D, Schlitterlau A et al. GABAergic modulation of DC stimulation-induced motor cortex excitability shifts in humans. *Eur J Neurosci* 2004; 19:2720–2726.
14. Nitsche MA, Lampe C, Antal A et al. Dopaminergic modulation of long-lasting direct current-induced cortical excitability changes in the human motor cortex. *Eur J Neurosci* 2006;23:1651–1657.
15. Monte-Silva K, Kuo MF, Liebetanz D, Paulus W, Nitsche MA. Shaping the optimal repetition interval for cathodal transcranial direct current stimulation (tDCS). *J Neurophysiol* 2010;103:1735–1740.
16. Nitsche MA, Doemkes S, Karaköse T et al. Shaping the effects of transcranial direct current stimulation of the human motor cortex. *J Neurophysiol* 2007;97:3109–3117.
17. Bikson M, Rahman A, Datta A. Computational models of transcranial direct current stimulation. *Clin EEG Neurosci* 2012;43:176–183.
18. Dasilva AF, Volz MS, Bikson M, Fregni F. Electrode positioning and montage in transcranial direct current stimulation. *Vis Exp* 2011;51:e2744.
19. Woods AJ, Bryant V, Sacchetti D, Gervits F, Hamilton R. Effects of electrode drift in transcranial direct current stimulation. *Brain Stimul* 2015;8:515–519.
20. Woods AJ, Antal A, Bikson M et al. A technical guide to tDCS, and related non-invasive brain stimulation tools. *Clin Neurophysiol* 2016;127:1031–1048.
21. Hummel F, Celnik P, Giraux P et al. Effects of non-invasive cortical stimulation on skilled motor function in chronic stroke. *Brain* 2005;128:490–499.
22. Bütefisch CM, Khurana V, Kopylev L, Cohen LG. Enhancing encoding of a motor memory in the primary motor cortex by cortical stimulation. *J Neurophysiol* 2004;91: 2110–2116.
23. Karok S, Witney AG. Enhanced motor learning following task-concurrent dual transcranial direct current stimulation. *PLoS One* 2013;8:e85693.
24. Chhatbar PY, Ramakrishnan V, Kautz S, George MS, Adams RJ, Feng W. Transcranial direct current stimulation post-stroke upper extremity motor recovery studies exhibit a dose-response relationship. *Brain Stimul* 2016;9:16–26.
25. Knotkova H, Leuschner Z, Soto E, Davoudzadeh E, Greenberg A, Cruciani R. Evaluating outcomes of transcranial direct current stimulation (tDCS) in patient with chronic neupathic pain. *J Pain* 2014;15:S69.
26. Knotkova H, Greenberg A, Soto E, Cruciani R. Applications of neuromodulation in pain management. In: *Textbook of neuromodulation*. New York: Springer, 2015:187–210.
27. Fregni F, Boggio PS, Lima MC et al. A sham-controlled, phase II trial of transcranial direct current stimulation for the treatment of central pain in traumatic spinal cord injury. *Pain* 2006;122:197–209.
28. Fregni F, Gimenes R, Valle AC et al. Randomized, sham-controlled, proof of principle study of transcranial direct current stimulation for the treatment of pain in fibromyalgia. *Arthritis Rheum* 2006;54:3988–3998.
29. Fenton BW, Palmieri PA, Boggio P, Fanning J, Fregni F. Preliminary study of transcranial direct current stimulation for the treatment of refractory chronic pelvic pain. *Brain Stimul* 2009;2:103–107.
30. Mori F, Codecà C, Kusayanagi H et al. Effects of anodal transcranial direct current stimulation on chronic neuropathic pain in patients with multiple sclerosis. *J Pain* 2010;11:436–442.
31. Roizenblatt S, Fregni F, Gimenez R et al. Site-specific effects of transcranial direct current stimulation on sleep and pain in fibromyalgia: a randomized, sham-controlled study. *Pain Pract* 2007;7:297–306.
32. Acler M, Bocci T, Valenti D, Turri M, Priori A, Bertolasi L. Transcranial direct current stimulation (tDCS) for sleep disturbances and fatigue in patients with post-polio syndrome. *Restor Neurol Neurosci* 2013;31:661–668.
33. Nitsche MA, Nitsche MS, Klein CC, Tergau F, Rothwell JC, Paulus W. Level of action of cathodal DC polarisation induced inhibition of the human motor cortex. *Clin Neurophysiol* 2003;114:600–604.
34. Klem GH, Lüders HO, Jasper HH, Elger C. The ten-twenty electrode system of the International Federation. The International Federation of Clinical Neurophysiology. *Electroencephalogr Clin Neurophysiol Suppl* 1999;52:3–6.
35. Charvet L, Kasschau M, Datta A et al. Remotely supervised transcranial direct current stimulation (tDCS) for clinical trials: guidelines for technology and protocols. *Front Syst Neurosci* 2015;9:1–13.
36. Datta A, Truong D, Minhas P, Parra LC, Bikson M. Inter-individual variation during transcranial direct current stimulation and normalization of dose using MRI-derived computational models. *Front Psychiatry* 2012;3:1–8.
37. Truong DQ, Magerowski G, Blackburn GL, Bikson M, Alonso-Alonso M. Computational modeling of transcranial direct current stimulation (tDCS) in obesity: impact of head fat and dose guidelines. *Neuroimage Clin* 2013;2:759–766.
38. Huang Y, Dmochowski JP, Su Y, Datta A, Rorden C, Parra LC. Automated MRI segmentation for individualized modeling of current flow in the human head. *J Neural Eng* 2013;10:066004.
39. Datta A, Bansal V, Diaz J, Patel J, Reato D, Bikson M. Gyri-precise head model of transcranial direct current stimulation: improved spatial focality using a ring electrode versus conventional rectangular pad. *Brain Stimul* 2009;2:201–207.
40. Seibt O, Brunoni AR, Huang Y, Bikson M. The Pursuit of DLPFC: non-neuronavigated methods to target the left dorsolateral pre-frontal cortex with symmetric bicephalic transcranial direct current stimulation (tDCS). *Brain Stimul* 2015;8:590–602.

